

ADVANCES IN THE STUDY OF ELECTRODE KINETICS \*

Christopher M.A. Brett  
*Departamento de Química, Universidade de Coimbra*  
*3000 Coimbra, Portugal*

Abstract

The transfer of electrons across the electrode-solution interface has long been the subject of much research, not only from a fundamental point of view, but also because of its importance in electrocatalysis and other reactions of industrial interest. Electron transfer is very often coupled with preceding or following chemical reactions, so that elucidation of the full reaction mechanism and kinetics is more complex. With the advent of hydrodynamic electrodes and, more recently, greatly improved ways of analysing electrical transients, significant developments in the study of electrode kinetics have occurred. These advances will be surveyed and future prospects indicated.

Introduction

The kinetics of electrode processes is a subject which has received much attention in the last thirty to forty years, not only because of a desire to understand the nature of the electron transfer and associated phenomena, but also because of its important practical applications in electrocatalysis and reactions of industrial interest<sup>1</sup>. As a result a number of review articles and monographs have appeared on the subject in recent years e.g. Refs 2-9.

In this article I shall focus on the methodology of electrode kinetics, and not on the numerous applications of any one electrochemical technique.

Significant advances were made with the development of the dropping

---

\* Plenary lecture held at the first Meeting of the Portuguese Electrochemical Society, Coimbra, Novembro 1984.

mercury electrode and solid hydrodynamic electrodes which give a steady-state or quasi-steady-state response.

More recently with the important advances in electronics and integrated circuit fabrication, there have been corresponding advances in the accuracy obtainable from transient or relaxation techniques, which can measure faster rate constants than the steady-state techniques.

Very important and useful information may be obtained from spectroscopy in conjunction with electrochemistry. In particular electrochemical esr for detection and characterisation of intermediates, ellipsometry, ESCA, vibrational spectroscopy and so on.<sup>10,11</sup> Photoelectrochemistry<sup>12</sup> and modified electrodes<sup>13</sup> are other areas where electrode kinetics is of fundamental importance. However these aspects will not be treated here.

After a short section on the principles used to extract kinetic and mechanistic information we will consider their application to steady-state and to transient techniques. Finally we will discuss transient techniques at hydrodynamic electrodes.

#### Fundamental Aspects

##### (i) Pathway of a Simple Electrode Reaction

Any description of electrode reactions has to explain a number of practical factors, in particular the position and shape of the voltammetric (current-potential) wave — the latter is very dependent on the electrochemical technique employed.

We can regard a simple electron transfer reaction at an electrode as involving the following steps:

- (i) Diffusion of the electroactive species from bulk solution to just outside the double layer (mass transfer).
- (ii) Reorganisation of the solvent in the vicinity of the electrode, adsorption of the electroactive species etc., to enable electron transfer to occur.
- (iii) Electron transfer.
- (iv) Inverse of step (ii) — relaxation of the double layer, desorption etc..
- (v) Diffusion of the product to bulk solution (mass transfer).

The electron transfer itself is very fast ( $\sim 10^{-16}$  s) and the electrochemical rate constants we measure involve the global effect of steps (ii) to (iv). Steps (i) and (v) may be described by a mass transfer coefficient (effectively a rate constant).

##### (ii) Mass Transfer<sup>14,15</sup>

Diffusion to the electrode surface is defined by the concentration gradient at the electrode surface

$$D \left( \frac{\partial c}{\partial z} \right)_{z=0} \cong D \frac{(c_{\infty} - c_0)}{\delta} = k'_D (c_{\infty} - c_0) \quad (1)$$

where we make the approximation of a linear concentration gradient.  $c_{\infty}$  is the concentration in bulk solution,  $c_0$  at the electrode surface and  $\delta$  is known as the diffusion-layer thickness. The mass transfer coefficient is  $k'_D$  and increases as the diffusion-layer thickness decreases, for example due to forced convection. Migration of the electroactive species to the electrode should also be taken into account; however, in most kinetic studies an excess of supporting (inert) electrolyte is added to minimise changes in the double layer structure due to migration. Nevertheless corrections do often have to be made<sup>3</sup>.

The mass-transfer equation, neglecting migration, is

$$\frac{\partial c}{\partial t} = D \nabla^2 c - \underline{v} \cdot \nabla c \quad (2)$$

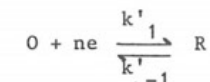
diffusion      convection

To this equation may have to be added extra terms describing the effect of coupled homogeneous reactions. Table I shows the convective-diffusion equation expressed in three different co-ordinate systems.

It should be noted that the solution to eqn. 2 depends on whether the fluid flow is laminar, in the transition regime, or turbulent. Virtually all kinetic studies have been conducted under laminar flow conditions, so we shall only consider this type of flow.

##### (iii) Electron Transfer

The rate of electron transfer is normally expressed in the Butler-Volmer formulation, which is a direct deduction from absolute rate theory. For the electrode process



we have

$$k'_1 = k'_0 \exp \left[ -\alpha \frac{nF(E - E^{\ominus})}{RT} \right] \quad (3a)$$

$$k'_{-1} = k'_o \exp \left[ (1-\alpha) \frac{nF(E-E^\ominus)}{RT} \right] \quad (3b)$$

$k'_o$  is the standard rate constant and  $\alpha$  the charge transfer coefficient. This refers to the whole electrode process and the value of  $\alpha$  is always fractional. If the electrode process contains two or more steps the value of  $\alpha$  may be misleading in terms of kinetic and mechanistic interpretation, as noted by some authors.<sup>4,16</sup> In general the transition state for a simple one-electron transfer lies approximately halfway between O and R leading to  $\alpha \approx 0.5$ .

(iv) Mass Transfer vs. Electron Transfer

What we actually observe in an electrochemical experiment depends critically on the relative values of  $k'_D$  and  $k'_o$ . There are clearly two extremes, when either  $k'_D$  or  $k'_o$  is rate determining.

When  $k'_D \ll k'_o$  the electrode reaction will be controlled by mass transfer at all points on the current-potential wave. This means that thermodynamic equilibrium is achieved at the electrode surface and that the Nernst equation can be applied. When all the electroactive species are being consumed at the interface, we observe the diffusion-limited current  $i_L$  ( $c_o = 0$  in eqn. 1). This is the reversible case and no information can be extracted with regard to the electrode kinetics.

When  $k'_o \ll k'_D$ , however, we have to apply a significant overpotential in order to cause a current to flow: near the equilibrium potential the current will be zero. When the current begins to rise from zero it will be purely kinetically controlled; as we go further up the wave  $k'_D$  eventually becomes smaller than  $k'_1$  (or  $k'_{-1}$ ) and we reach the diffusion-limited current  $i_L$ . This is the irreversible case. Oxidation and reduction waves are completely separated (by 100 mV or more) and the voltammetric wave is more drawn out than in the reversible case.

Many electrode processes lie between the two extremes. For all but reversible processes we can extract some kinetic information. Thus we have to choose the correct electrochemical technique so that  $k'_D$  is sufficiently large. In general, transient techniques can lead to the measurement of faster rate constants than steady-state techniques, owing to the very large  $k'_D$  values at short times (viz. homogeneous kinetics).

If we combine eqns 3a and 3b we obtain the Butler-Volmer equation

$$i = i_o \left[ \exp(-\alpha n F \eta / RT) - \exp\{(1-\alpha) n F \eta / RT\} \right] \quad (4)$$

$$\text{with } i_o = nFA k'_o c_{o,0}^{(1-\alpha)} c_{o,R}^\alpha$$

$$\frac{\partial c}{\partial t} = D \nabla^2 c - v \nabla c$$

in various coordinate systems

Table I. The Convective-Diffusion Equation

	Diffusion	Convection
Cartesian	$\frac{\partial c}{\partial t} = D \left[ \frac{\partial^2 c}{\partial x^2} + \frac{\partial^2 c}{\partial y^2} + \frac{\partial^2 c}{\partial z^2} \right]$	$- \left[ v_x \frac{\partial c}{\partial x} + v_y \frac{\partial c}{\partial y} + v_z \frac{\partial c}{\partial z} \right]$
Cylindrical	$\frac{\partial c}{\partial t} = D \left[ \frac{1}{r} \frac{\partial}{\partial r} \left( r \frac{\partial c}{\partial r} \right) + \frac{1}{r^2} \frac{\partial^2 c}{\partial \phi^2} + \frac{\partial^2 c}{\partial z^2} \right]$	$- \left[ v_r \frac{\partial c}{\partial r} + \frac{v_\phi}{r} \frac{\partial c}{\partial \phi} + v_z \frac{\partial c}{\partial z} \right]$
Spherical polar	$\frac{\partial c}{\partial t} = D \left[ \frac{1}{r^2} \frac{\partial}{\partial r} \left( r^2 \frac{\partial c}{\partial r} \right) + \frac{1}{r^2 \sin^2 \theta} \frac{\partial^2 c}{\partial \phi^2} + \frac{\sin \theta}{\partial \theta} \frac{\partial c}{\partial \theta} + \frac{1}{r^2 \sin^2 \theta} \frac{\partial^2 c}{\partial \phi^2} \right]$	$- \left[ v_r \frac{\partial c}{\partial r} + \frac{v_\theta}{r} \frac{\partial c}{\partial \theta} + \frac{v_\phi}{r \sin \theta} \frac{\partial c}{\partial \phi} \right]$

where  $i_0$  is the exchange current defined for  $E = E_{eq}$ , and we are assuming that surface and bulk concentrations are equal. It is easy to see that when either the forward or the backward reaction can be neglected then

$$E \propto \log i + \text{constant} \quad (5)$$

a relationship found experimentally by Tafel. Thus a plot of  $E$  vs.  $\log i$ , a Tafel plot, can lead, as shown in Fig. 1, to values of  $E_{eq}$ ,  $E^\ominus$  and  $\alpha$ . Tafel plots can be corrected for concentration changes in the vicinity of the electrode by plotting  $E$  vs  $\ln \frac{i_L - i}{i}$ , enabling use of the whole voltammetric wave for analysis.<sup>17</sup>

When there is multiple electron transfer, for example a two-step (EE) process, the form of the  $i$ - $E$  characteristic will depend on whether the second electron transfer is easier than the first or not. Methods have been devised based on logarithmic plots, principally at the DME, in analysing these waves and allowing their deconvolution.<sup>18</sup>

(v) Coupled Homogeneous Reactions

Many electrode processes, particularly those involving organic compounds, are coupled with homogeneous reactions preceding or following the electron transfer: Table II shows some of the more commonly encountered types of reaction scheme together with an example of each kind.

It is helpful to think of a reaction layer within which the concentrations of the species reacting homogeneously are perturbed from their equilibrium values in the absence of reaction. The faster the homogeneous reaction, the thinner will be the reaction layer. If it is significantly thinner than the diffusion layer, then the electrochemical and chemical steps can be separated, which simplifies the mathematical treatment. If the two layers are of roughly the same thickness then such a simplification is not possible.

At microelectrodes, because of their small size, the effect of coupled homogeneous reactions is small (reaction layer much thicker than the diffusion layer).<sup>19</sup> A comparison between experimental results obtained at micro- and at macro-electrodes should facilitate the elucidation of complex electrode processes.

Another interesting recent development is that of the vibrating dropping mercury electrode which produces regular, uniform drops down to drop times as short as 5 ms.<sup>20</sup> Once again the diffusion layer is much smaller than the reaction layer. In this case a comparison is made

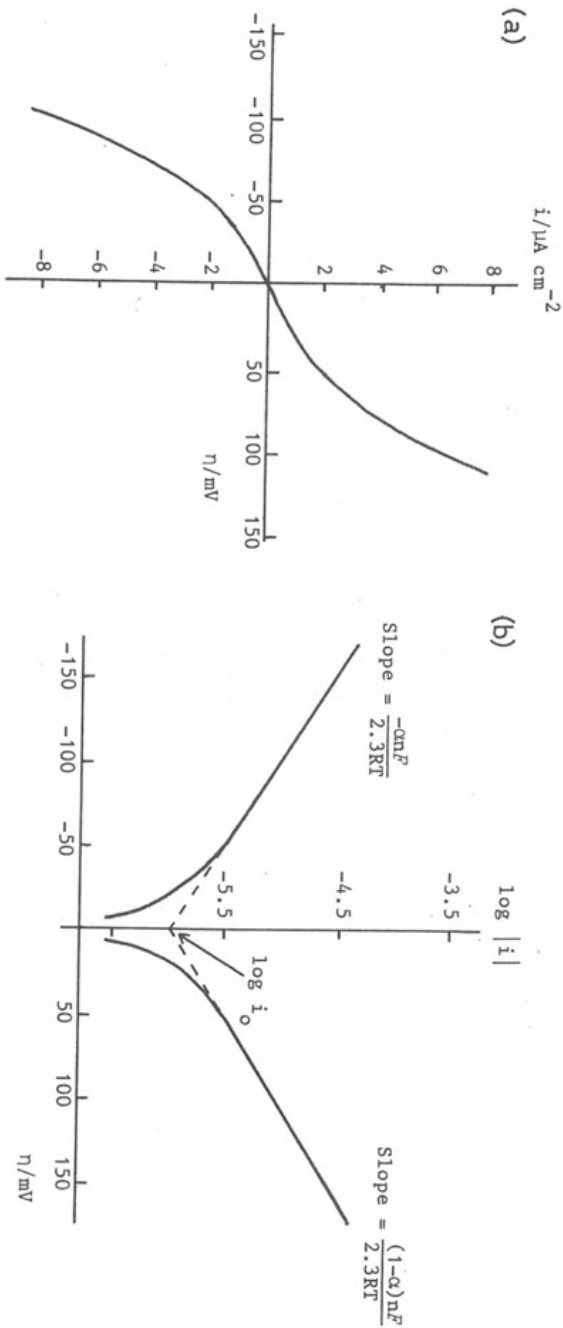


Fig. 1 (a) Plot of current vs. overpotential for an irreversible electron transfer with  $i_0 = 10^{-6} \text{ A cm}^{-2}$  and  $\alpha = 0.5$  in the region of the equilibrium potential.

(b) Tafel plot corresponding to (a) showing extraction of  $i_0$  (and hence  $k_0^1$ ),  $E_{eq}$  and  $\alpha$ .

Table II. Common Examples of Electron Transfer with Coupled Homogeneous Chemical Reactions

Electrode Process	Example
<p>Preceding Chemical (CE)</p> <p>e.g. Solution <math>A_2 \xrightleftharpoons[k_{-1}]{k_1} A_1</math></p> <p>Electrode <math>A_1 \pm ne \rightarrow A_3</math></p>	<p><math>A_2 = H_2C(OH)_2</math></p> <p><math>A_1 = H_2CO</math></p> <p><math>A_3 = CH_3OH</math></p>
<p>Parallel/catalytic (EC')</p> <p>e.g. Solution <math>A_2 \xrightleftharpoons[k_{-1}]{k_1} A_1</math></p> <p>Electrode <math>A_1 \pm ne \rightarrow A_2</math></p>	<p><math>A_2 = Fe(III)</math></p> <p><math>A_1 = Fe(II)</math></p> <p>'Catalyst' = <math>H_2O_2</math></p>
<p>Following Chemical (EC)</p> <p>e.g. Electrode <math>A_3 \pm ne \rightarrow A_1</math></p> <p>Solution <math>A_1 \xrightleftharpoons[k_{-1}]{k_1} A_2</math></p>	<p><math>A_3 = R_2N-\text{C}_6\text{H}_4-NR_2</math></p> <p><math>A_1 = R_2N^+-\text{C}_6\text{H}_4-NR_2^+</math></p> <p><math>A_2 = O=\text{C}_6\text{H}_4=O</math> by reaction with <math>OH^-</math></p>
<p>Following Chemical (ECE)</p> <p>e.g. Electrode <math>A_3 \pm n_1e \rightarrow A_1</math></p> <p>Solution <math>A_1 \xrightarrow{k} A_2</math></p> <p>Electrode <math>A_2 \pm n_2e \rightarrow A_4</math></p>	<p><math>A_3 = ClC_6H_4NO_2</math></p> <p><math>A_1 = ClC_6H_4NO_2^-</math></p> <p><math>A_2 = \cdot C_6H_4NO_2</math></p> <p><math>A_4 = \cdot C_6H_4NO_2</math></p> <p><math>(A_4 + H^+ \rightarrow C_6H_5NO_2)</math></p>

between results obtained at short and at long drop times.

(vi) Theoretical Models

Once we have found a technique such that we can obtain kinetic and mechanistic information, in order to calculate rate constants etc. correctly we have to fit the experimental results to a theoretical model. For a simple electron transfer or other simple mechanism the model probably already exists. If it does not then we have to set up the convective-diffusion equations with extra kinetic terms if necessary and solve them with the appropriate boundary conditions. This is nearly always most conveniently performed in Laplace space by making use of the Laplace transformation.<sup>21</sup> However, inversion of the result into real space can be difficult. In order to obtain an analytical solution approximations are often necessary. Alternatively we can use numerical techniques, but these, of course, also involve approximations.

Instead of analytical or numerical techniques, or as a complement to them, we can use digital simulation,<sup>22,23</sup> which was pioneered by Feldberg. It is particularly useful in cases not amenable to analytical or numerical techniques. With the increasing power and availability of computers, digital simulation is becoming very widespread, and indeed, can nearly always be performed on a modern microcomputer.

It should be remembered that several mechanisms may lead to virtually the same (experimental) response. If there is some doubt, then it may be opportune to use two or more different electrochemical techniques to characterise the reaction completely and correctly.

Steady-State Techniques<sup>24</sup>

For steady-state techniques we put  $\partial c/\partial t=0$  in the convective-diffusion equation (eqn. 2). However we shall also include dc polarography in this category where  $\partial c/\partial t$  varies in a cyclic fashion. In order to obtain a steady state it is necessary to have a constant diffusion layer thickness. This is achieved by imposing forced convection which not only keeps the thickness constant but also makes it rather small. By altering the rate of convection — rate of movement of the electrode or solution — we alter this thickness directly, and hence the mass transfer coefficient,  $k'_D$ . This gives us another controlling parameter in kinetic studies. Electrodes under forced convection are known as hydrodynamic electrodes, and their development owes much to Levich.<sup>14</sup>

The most widely used solid hydrodynamic electrodes for kinetic stu-

dies are the rotating disc electrode (RDE)<sup>25-27</sup> and its double electrode analogue, the rotating ring disc electrode (RRDE)<sup>28-30</sup>. The particular advantages of double electrodes will be indicated below. The popularity of the RDE stems from the fact that under most conditions the electrode surface is uniformly accessible which simplifies resolution of the mathematical equations. Additionally the electrode is easily removed for polishing and maintenance.

The only other widely used uniformly accessible electrode, although this is a first approximation only, is the dropping mercury electrode (DME)<sup>31,32</sup>. The non-uniformity derives principally from shielding effects due to the capillary tip. Nevertheless it preceded the RDE by several decades and much of the early kinetic work was performed at the DME.<sup>33</sup> Although drop growth and consequent double layer charging are problems in its application, it does have the advantages that the surface presented to the solution is constantly renewed and that it has a large cathodic range.

In Table III are presented the solutions of the convective diffusion equation for the diffusion-limited current,  $i_L$ , at some common used hydrodynamic electrodes.

(i) Current-Voltage Curves

It is fairly easy to show that, for a reversible system involving only electron transfer, the equation describing the current-voltage curve is

$$E = E_{1/2}^r + \frac{RT}{nF} \ln \frac{i_L^c - i}{i - i_L^a} \quad (6)$$

where the reversible half-wave potential  $E_{1/2}^r$  is given by

$$E_{1/2}^r = E^\ominus + \frac{RT}{nF} \ln \left(\frac{D}{D_0}\right)^s \quad (7)$$

and  $s=1/2$  for the DME and  $s=2/3$  for all other hydrodynamic electrodes. In practice the ratio  $D_R/D_0$  is close to unity and we can usually make the assumption that  $E_{1/2}^r = E^\ominus$ . We conclude that for a reversible wave

- (i)  $E_{1/2}^r$  is independent of  $[O]_\infty$  and  $[R]_\infty$ .
- (ii) The wave shape is independent of the rate of convection.
- (iii) A plot of  $\log [(i_L^c - i)/(i - i_L^a)]$  vs.  $E$  gives a straight line of slope  $0.0591/n$  V at 298K and crosses zero at  $E = E_{1/2}^r$ .

Table III. Diffusion-limited currents,  $i_L$ , at some common hydrodynamic electrodes.<sup>a</sup>

		Ref
Rotating Disc <sup>b,c</sup>	$i_L = 1.554 nF c_\infty D^{2/3} \nu^{-1/6} \pi r_1^2 \omega^{1/2}$	25
Dropping Mercury <sup>b</sup> (Ilkovič Equation)	$i_L = 709 n c_\infty D^{1/2} m_1^{2/3} t^{1/6}$ (instantaneous current) $i_L = 607 n c_\infty D^{1/2} m_1^{2/3} \tau^{1/6}$ (average current)	34
Wall Tube <sup>b,c</sup>	$i_L = 1.53 nF c_\infty D^{2/3} \nu^{-1/6} \pi r_1^2 (V_F/r_1^3)^{1/2}$	35
Tube	$i_L = 5.43 nF c_\infty D^{2/3} x^{2/3} V_F^{1/3}$	36
Channel	$i_L = 0.925 nF c_\infty D^{2/3} (h^2 d)^{-1/3} w x^{2/3} V_F^{1/3}$	36
Wall-Jet <sup>c</sup>	$i_L = 1.38 nF a^{-1/2} c_\infty D^{2/3} \nu^{-5/12} r_1^{3/4} V_F^{3/4}$	37,38

<sup>a</sup> For meaning of symbols see end of text

<sup>b</sup> Uniformly accessible

<sup>c</sup> The  $i_L$  expression for the ring-electrode analogue is obtained by replacing  $r_1^n$  with  $(r_3^{3n/2} - r_2^{3n/2})^{2/3}$

The general case is, of course, more complicated. We have to consider the competing effects of electron transfer and mass transfer rates. At uniformly accessible electrodes we can obtain exact expressions. In particular, for a first order reaction we find

$$\frac{1}{i} = \frac{1}{i_k} + \frac{1}{i_L^c} \quad (8)$$

for a reduction where

$$i_k = n F A k'_1 [O]_\infty \quad (9)$$

Thus taking the example of the RDE<sup>39</sup>, a plot of  $i^{-1}$  vs.  $W^{-1/2}$  will enable us to determine  $D$  and  $k'_1$  as shown in Fig. 2, providing the values for all

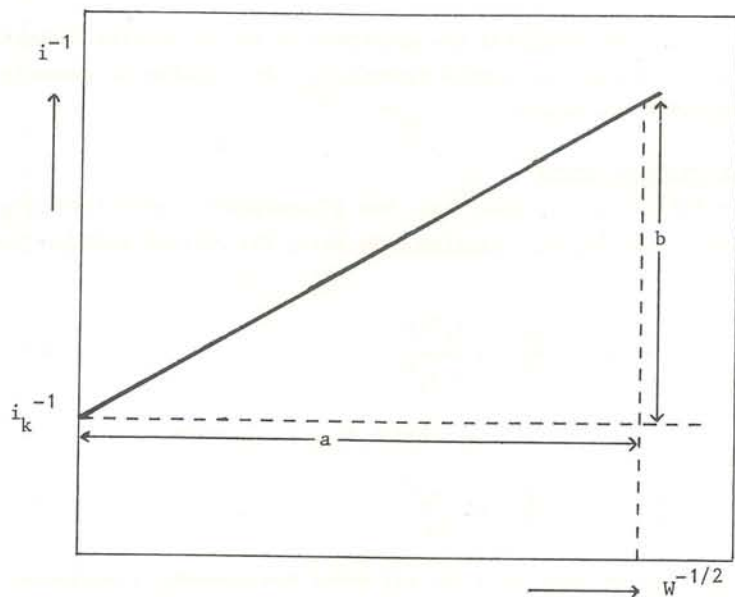


Fig. 2 Plot of  $i^{-1}$  vs.  $W^{-1/2}$  at the RDE for a non-reversible reduction with  $i < i_L^c$  showing measurement of  $i_k$  (Eqn.9). The diffusion coefficient may be calculated from the slope of the plot. [Note that  $i_L^c = (a/b)W^{1/2}$ ].

the other variables are known. Reactions do occur where, owing to adsorption in particular, the order is fractional: analysis can be performed most easily by a graphical method<sup>40</sup>.

At non-uniformly accessible electrodes, to obtain an analytical or numerical solution for the current-voltage curve we have to make approximations. Matsuda and co-workers arrived at the following generic approximate expression for current-voltage curves at a number of different hydrodynamic electrodes. The form of these is

$$i = \left[ \frac{i_L^c}{1+e^\xi} + \frac{i_L^a}{1+e^{-\xi}} \right] \cdot \frac{k'_o/D^s \sigma (e^{-\alpha\xi} + e^{(1-\alpha)\xi})}{A + k'_o/D^s \sigma (e^{-\alpha\xi} + e^{(1-\alpha)\xi})} \quad (10)$$

where

$$\xi = \frac{nF}{RT} (E - E_{1/2}^r) \quad (10a)$$

$$D = D_0^{1-\alpha} D_R^\alpha \quad (10b)$$

$$s = 1/2 \text{ (DME); } s = 2/3 \text{ in all other cases}$$

and where  $\sigma$  is a mass transport dependent expression and  $A$  is a number which is a constant for a uniformly accessible electrode, but which in other cases depends on the electrode geometry and has been numerically evaluated. Values of  $\sigma$  and  $A$  are to be found in Table IV. Note that when

$$A \ll k'_o/D^s \sigma (e^{-\alpha\xi} + e^{(1-\alpha)\xi}) \quad (11)$$

we obtain the reversible case (eqn. 6).

An interesting and useful conclusion from this is that since we have a generic expression for uniformly accessible and non-uniformly accessible electrodes the type of analysis performed at the RDE<sup>39</sup> may be used within a small error of about 2% at other hydrodynamic electrodes in order to calculate standard rate constants. This error will manifest itself most as we approach the limiting current  $i_L$ ; at the foot of an irreversible wave we have pure kinetic control and therefore uniform accessibility for all electrodes: the non-uniformity increases as the current increases.

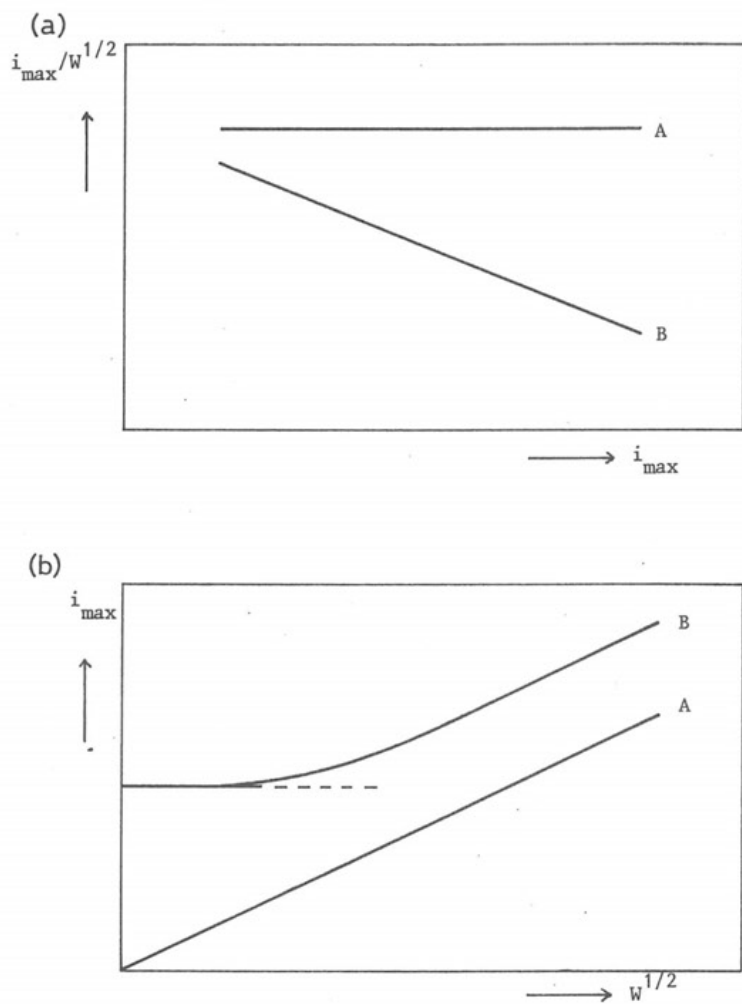


Fig. 3 Diagnostic plots for coupled homogeneous reactions  
 (a) CE mechanism. A: no effect from preceding chemical reaction ( $i_{\max} = i_L$ ). B: showing effect of preceding chemical reaction ( $i_{\max} < i_L$ ).  
 (b) EC' mechanism. A: no catalytic reaction ( $i_{\max} = i_L$ ). B: with catalytic reaction ( $i_{\max} > i_L$ ).

Table IV. Current-voltage curve parameters for some hydrodynamic electrodes according to equation 10<sup>a</sup>.

	$\sigma$	A	Ref.
Rotating Disc	$v^{1/6} \omega^{-1/2}$	0.620	41
Rotating Ring	$v^{1/6} \omega^{-1/2}$	0.620 B(r)	42
Ring of RRDE (reactant produced at disc)	$v^{1/6} \omega^{-1/2}$	0.799 C(r, $E_R$ )	43 (see also 44)
Tube	$V_E^{-1/3} R x_1^{1/3} \tau^{-1/2}$	0.839	45 (see also 46)
DME (expanding plane model) <sup>c</sup>	$\tau^{-1/2}$	1.13	47

<sup>a</sup> For meaning of symbols see end of text

<sup>b</sup> Note that values of A are approximate except for the RDE; B is a function of r and C a function of both r and ring potential

<sup>c</sup> In eqn. 10, D is raised to the power 0.5

(ii) Multistep Processes at Single Electrodes

Multiple processes may involve multiple electron transfer or coupled homogeneous reactions or both. We now consider the effects of various types of homogeneous coupled reactions on the steady-state voltammetric wave.

In a preceding chemical (CE) mechanism the concentration of electro-active species is less than it would be in a simple electron transfer mechanism. The diffusion-limited current will not be reached, but instead we register a smaller value  $i_{\max}$ ; the position of the wave on the potential axis remains unaltered. For example at the RDE, as the rotation speed is increased  $i_{\max}$  will not increase proportionally to  $\omega^{1/2}$  owing to the limiting effect of the preceding chemical step. We thus register a plot of the type shown in Fig. 3a; analysis of this leads to the values of the homogeneous rate constants<sup>24</sup>.

In the case of the parallel/catalytic (EC') mechanism the limiting currents measured are larger than  $i_L$ . When the reaction layer thickness is much smaller than the diffusion layer thickness, the value of  $i_{\max}$  is independent of convection rate (fast chemical step). As the convection rate is further increased the thicknesses become comparable and a convective rate dependence arises (Fig. 3b).

For the following chemical (EC or ECE) mechanism there is a more complex behaviour. The product of the electron transfer has its concentration reduced by the chemical reaction resulting in a shift in the position of the voltammetric wave: anodic waves to more negative potentials and cathodic waves to more positive potentials. Kinetic parameters may often be obtained directly from these shifts in the half-wave potential. Note that in these cases  $i_{\max} = i_L$ .

(iii) Multistep Processes at Double Electrodes

Double electrodes are invaluable in the elucidation of mechanisms involving at least two electrochemical steps, perhaps with an interposed chemical step e.g. EE, ECE etc., when we can arrange for the first electrochemical step to occur at the upstream electrode and the second at the downstream electrode.

An important parameter at hydrodynamic double electrodes is the steady-state collection efficiency,  $N_0$ . It is defined as the ratio between the Faradaic current at the downstream electrode to that at the upstream electrode for a simple system without homogeneous reaction. Since some of the reaction product from the upstream electrode escapes into bulk

solution, its value will always be less than unity. The expression is

$$N_0 = 1 - F(\alpha/\beta) + \beta^{2/3} \{1 - F(\alpha)\} - (1 + \alpha + \beta)^{2/3} [1 - F\{(\alpha/\beta)(1 + \alpha + \beta)\}] \quad (12)$$

where

$$F(\theta) = \frac{3^{1/2}}{4\pi} \ln \left\{ \frac{(1 + \theta^{1/3})^3}{1 + \theta} \right\} + \frac{3}{2\pi} \tan^{-1} \left( \frac{2\theta^{1/3} - 1}{3^{1/2}} \right) + 1/4 \quad (13)$$

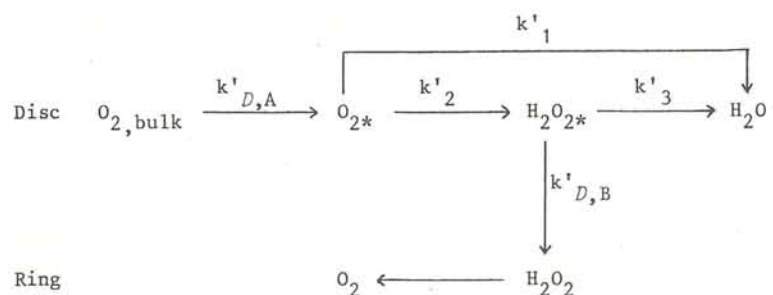
and  $\alpha$  and  $\beta$  have different values, dependent solely on electrode geometry, according to the system under consideration, as shown in Table V. Thus  $N_0$ ,

Table V. Values of the geometric parameters  $\alpha$  and  $\beta$  for common hydrodynamic electrodes (see equation 12)

	$\alpha$	$\beta$
Rotating ring-disc Wall-tube ring-disc	$\left(\frac{r_2}{r_1}\right)^3 - 1$	$\frac{r_3^3}{r_1^3} - \left(\frac{r_2}{r_1}\right)^3$
Wall-jet ring-disc	$\left(\frac{r_2}{r_1}\right)^{9/8} - 1$	$\frac{r_3^{9/8}}{r_1^{9/8}} - \left(\frac{r_2}{r_1}\right)^{9/8}$
Double tube Double channel	$\frac{x_2}{x_1} - 1$	$\frac{x_3}{x_1} - \frac{x_2}{x_1}$

being a function purely of electrode geometry, is independent of fluid flow. Values of  $N_0$  are often chosen to be around 0.2.

In the case of consecutive or parallel electron transfer, or branching mechanisms it is relatively simple to calculate the relation between currents at upstream and downstream electrodes. A very important application of this is the considerable amount of research conducted into the electroreduction of oxygen at the RRDE, principally, and until recently, by Bockris et al. and the Soviet school.<sup>48</sup> We take this as an illustrative example. A probable mechanism at platinum electrodes is



where the ring potential is set such that all  $H_2O_2$  reaching it is oxidised. Making the stationary-state assumptions precisely in the same way as for an analogous homogeneous kinetics scheme we eventually arrive at the following expressions

$$N_o \frac{i_D}{i_R} = [1 + 2 \frac{k'_1}{k'_2}] + \frac{2(k'_1/k'_2 + 1)k'_3}{k'_{D,B}} \quad (14)$$

$$\frac{i_{D,L}}{i_{D,L} - i_D} = 1 + \frac{k'_1 + k'_2}{k'_{D,A}} \quad (15)$$

which allow the determination of  $k'_1, k'_2$  and  $k'_3$ . If we plot  $i_D/i_R$  vs  $W^{-1/2}$  (eqn. 14) we will obtain lines of different positive slopes depending on the applied potential at the disc and thus the relative values of  $k'_1, k'_2$  and  $k'_3$ . For example, if  $k'_1$  and  $k'_3$  are both very small then the slope of the plot will be zero and its intercept  $N_o^{-1}$ .

In the investigation of ECE and similar mechanisms we can define kinetic collection efficiencies  $N_k$ , which will depend on whether the chemical step is first or second order, and on the rate of the homogeneous reaction. In this way first order homogeneous rate constants up to  $10^3 \text{ s}^{-1}$  and second order up to  $10^8 \text{ dm}^3 \text{ mol}^{-1} \text{ s}^{-1}$  have been measured at the RRDE<sup>49</sup>. At the double channel electrode, the range of measurable rate constants is very similar<sup>50,51</sup>.

Transient Techniques

Transient or relaxation techniques offer the possibility of measuring faster rate constants than in the steady-state. However the double layer charging contribution to the total current has to be separated out. Various ways can be used to achieve this object as will be seen below. Table VI shows some of the transient techniques commonly employed.

Table VI. Transient Techniques for Studying Electrode Processes

<p>A. Potential Perturbation (Potentiostatic techniques)</p> <p>(a) Single potential step</p> <p>(b) Multiple potential step i.e. pulse techniques</p> <p>(c) Linear Sweep/Cyclic Voltammetry</p> <p>(d) Ac impedance — without dc potential bias — with dc potential bias/ramp</p>
<p>B. Current Perturbation (Galvanostatic techniques)</p> <p>(a) Single current step</p> <p>(b) Multiple current step</p> <p>(c) Ac impedance</p>

(i) Potential and Current Step

These two techniques are the basis for all the others in Table VI. For a potential step we are usually interested in the variation of current with time (chronoamperometry) and for a current step the variation of potential with time (chronopotentiometry). Fig. 4 shows schematically, these variations and the effect of the double layer charging current.

The Faradaic current obtained for a potential step under mass-transfer control is given by the Cottrell relation<sup>52</sup>

$$i_t = nFA c_\infty D^{1/2} (\pi t)^{-1/2} \quad (16)$$

The diffusion-layer thickness increases with  $t^{1/2}$ . Thus after a certain value of  $t$  (usually around 1s) natural convection etc. will disrupt the diffusion layer and the relation is no longer applicable. It is interesting the Ilković equation at the DME was derived by modifying the Cottrell relation for drop growth<sup>34</sup>.

When we are considering a quasi-reversible or irreversible process then application of a potential step will not give the  $i-t$  behaviour described by equation 16. If we consider an irreversible reaction then it can be shown that as  $t \rightarrow 0$ ,  $i \rightarrow i_k$  and at short times

$$i = nFA k'_1 c_\infty [1 - 2k'_1 t^{1/2} (\pi D)^{-1/2}] \quad (17)$$

for a reduction. The corresponding expression for a quasi-reversible

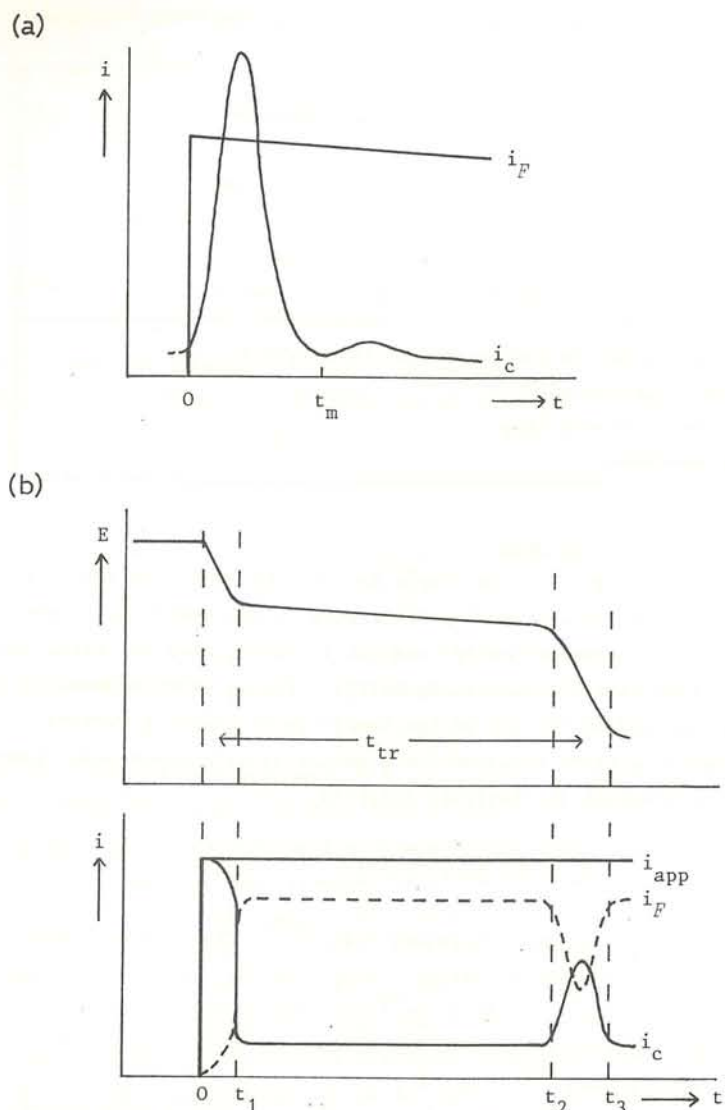


Fig. 4 (a) Schematic representation of current response to potential step at a reversible electrode. After  $t=t_m$  (a few  $\mu s$  with high quality i.c.'s)  $i_c$  (capacitative current) can be neglected with respect to  $i_F$  (Faradaic current).  
 (b) Schematic representation of current and potential response to an applied current step ( $i_{app}$ ).

reaction is, naturally, more complex. Note that at very short times the total current will be dominated by the double layer contribution and so we have to use an extrapolation procedure. Extraction of rate constants, transfer coefficients and so on and the equations applicable to analysis of coupled homogeneous reactions have been described.<sup>53</sup>

The fundamental equation for a current step under mass-transfer control is the Sand equation<sup>54</sup>

$$i = \frac{1}{2} nFAc_{\infty} (\pi D)^{1/2} t_{tr}^{-1/2} \quad (18)$$

where  $t_{tr}$  is the time during which the potential is roughly constant during the occurrence of a particular Faradaic process (see Fig. 4). Expressions for the analysis of kinetically controlled electron transfer and for coupled homogeneous reactions have been derived<sup>55</sup>. In particular for an irreversible electron transfer it can be shown that a plot of  $E$  vs.  $\ln[1-(t/t_{tr})^{1/2}]$  is linear with slope  $RT/\alpha nF$  for a reduction;  $E(t=0)$  by extrapolation is related directly to the standard rate constant.

Pulse techniques can be regarded as a succession of potential or current steps; theoretical analysis is along these lines. We now turn to consider linear sweep/cyclic voltammetry and ac impedance techniques.

(ii) Linear Sweep/Cyclic Voltammetry

In these techniques the potential of a stationary electrode is varied linearly with time. Cyclic voltammetry (CV) differs from linear sweep voltammetry (LSV) only in that the initial potential sweep is reversed, enabling intermediates or products formed during the initial scan to be detected. Scan rates may range from a few mV per hour (corresponding to a steady-state response with its associated natural convection problems etc.) to tens or hundreds of volts per second.

The shape of the linear sweep voltammogram may be described in two parts. First a steep rise in current due to the exponential term in the electron transfer rate constant. Second, as concentration depletion at the electrode surface occurs the diffusion layer thickness increases with  $t^{1/2}$  and the current drops accordingly. The detailed shape will depend on the complexity of the electrode process, coupled homogeneous reactions and so on. CV is particularly useful in mechanistic investigations owing to the fact that the initial potential affects the reaction products formed.

For a simple electron transfer the relations describing the systems

are

(a) Reversible

$$E_p = E_{1/2} \pm \frac{0.0285}{n} \quad (19)$$

$$i_p = 2.67 \times 10^5 n^{3/2} A D^{1/2} c_\infty v^{1/2}$$

so that  $E_{p,0} - E_{p,R} = 0.057V$

(b) Irreversible

$$(E_p)_2 - (E_p)_1 = \frac{RT}{\alpha n_a F} \ln (v_1/v_2)^{1/2} \quad (20)$$

$$i_p = 3.01 \times 10^5 n (\alpha n_a)^{1/2} A D^{1/2} c_\infty v^{1/2}$$

where  $n_a$  is the number of electrons transferred in the rate determining step and subscripts 1 and 2 refer to different scan rates.

In these expressions the peak current  $i_p$  varies with the square root of the scan rate,  $v$ , and the peak potential  $E_p$  varies with scan rate for the irreversible process. It is fairly obvious that a system which is reversible at low scan rates may appear irreversible at very high scan rates. The original work of Nicholson and Shain gives details on how to obtain the kinetic parameters from this and more complex processes<sup>56,57</sup>.

There are three important disadvantages of LSV and CV. The first has been largely overcome with modern instrumentation which was the delay between application of a potential to the potentiostat and its appearance at the electrodes plus the registering of accurate and instantaneous current responses; it is now possible to go to higher scan rates than before. The second is that the double layer current increases with scan rate whereas the faradaic current only increases with  $v^{1/2}$ .

The third disadvantage is based on the fact that we only use  $E_p$  and  $i_p$  for analysis purposes. It is easy to make significant errors in the measurement of  $i_p$ , particularly as it is often not clear where to draw the baseline — it is very rarely horizontal. For these reasons and in order to make use of the whole wave, Saveant et al have developed convolution potential sweep voltammetry (CPSV)<sup>58</sup> and Oldham et al semi-integral techniques<sup>59,60</sup>, methods which are essentially equivalent. As a result of these on-line transformations a sigmoid-type  $i$ - $E$  characteristic is produced which is very similar to a steady-state voltammogram (see Fig. 5). As

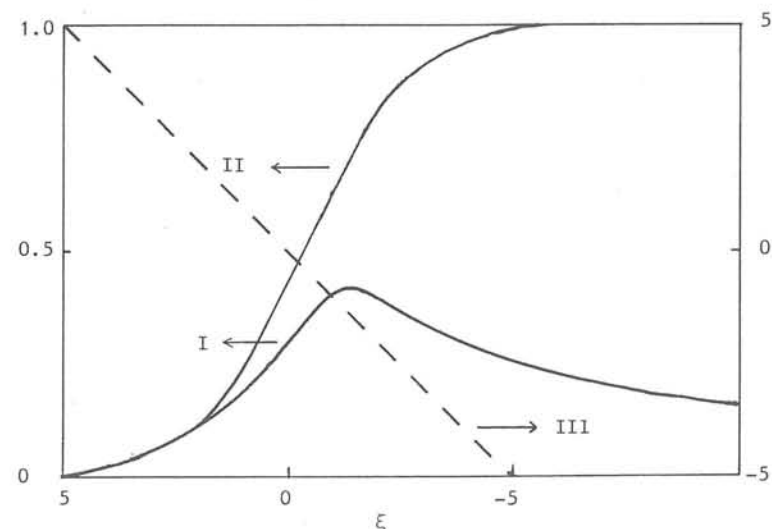


Fig. 5 Convolution potential sweep voltammetry. Plot of normalised current function (curve I), convoluted current function (curve II) and the logarithmic function (curve III).<sup>58</sup>

for steady-state voltammograms logarithmic analysis of the whole wave may be performed, reducing possible errors. This has been extended to include a large number of coupled homogeneous reaction schemes.

(iii) Impedance Methods<sup>61,62</sup>

By applying a time varying excitation signal to an electrochemical cell it is always possible, in principle, to separate the resistive and capacitive current contributions owing to their phase differences in the response signal. This is most easily and normally performed using a sinusoidal perturbation. Clearly the method is important not only for electrode kinetic studies but also for those of the double layer. Impedance bridges, frequency response analysers or lock-in amplifiers are used to measure the response. We are essentially interested in the Faradaic impedance. By separating out the double layer contribution we increase sensitivity which is used to good effect in ac polarography.

For a simple charge transfer we can draw the equivalent circuit of an electrochemical cell as shown in Fig. 6a. It consists of a resistan-

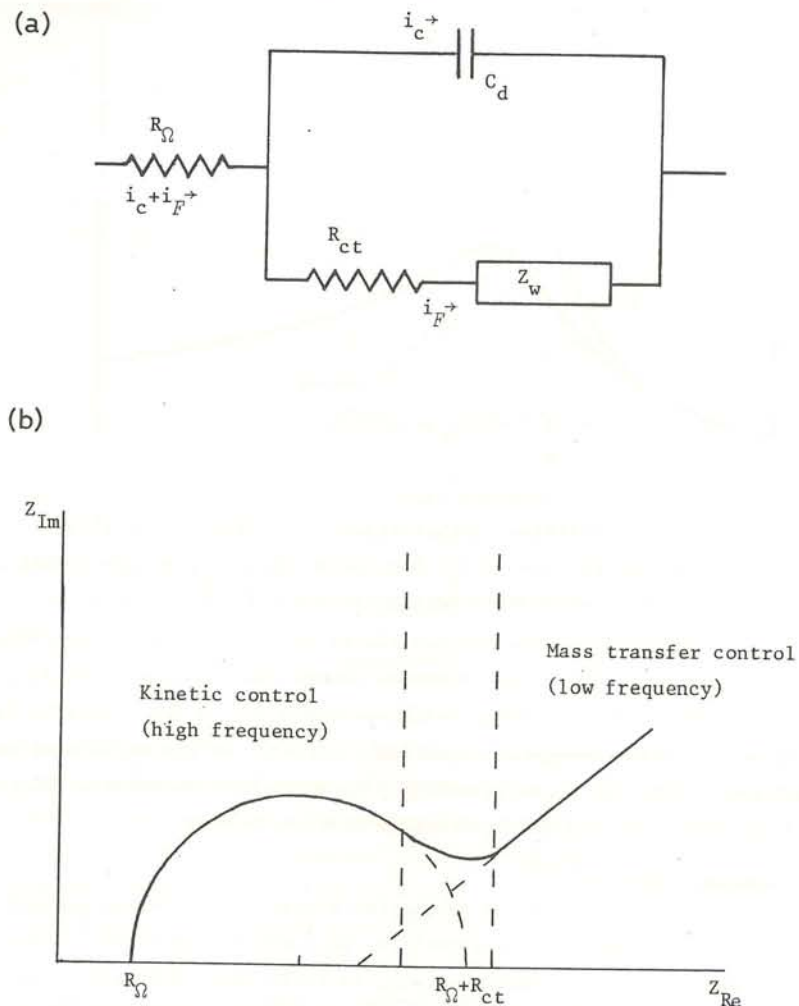


Fig. 6 Schematic representation of ac impedance.  
 (a) Electrical equivalent circuit of electrochemical cell.  
 (b) Corresponding impedance plot. See text for explanation.

ce to charge transfer,  $R_{ct}$ , a resistance to mass transfer, the Warburg impedance,  $Z_w$ , the double layer capacity  $C_d$  and the cell resistance  $R_\Omega$ . What is important for the understanding of the working of this circuit is whether at a given frequency we allow the system sufficient time to reach equilibrium, and also the effect of double layer capacity. The two extremes are

- (a) Low frequency. The system reaches equilibrium and we are under mass transfer control i.e.  $R_{ct} \ll Z_w$ . Also  $C_d$  is unimportant.
- (b) High frequency. Equilibrium is not reached and we are under kinetic control i.e.  $R_{ct} \gg Z_w$ .  $C_d$  is now very important.

Note that

$$R_{ct} = \frac{RT}{nF i_0} \quad Z_w \propto \omega^{-1/2} \quad (21)$$

We obtain the behaviour shown in Fig. 6b.

We can draw equivalent circuits for any electrode process involving adsorption, coupled homogeneous reactions and so on. Very often one finds semicircles corresponding to each successive step in the mechanism adjoining one another on the Argand diagram. Once more we have to be very careful with the problem of the incorrect theoretical circuit leading to the correct response. Despite these difficulties impedance techniques have found wide application in electrode kinetics, particularly for corrosion studies.

It is interesting to consider at this point the simultaneous application of signals of many different frequencies and the consequent time-saving in the calculation of the impedance plot over the entire frequency range. This may be achieved by, for example, the Fourier transform which is very widely used in spectroscopy. This transform is the most obvious to use as it is a special case of the Laplace transform which is encountered so often in the resolution of electrochemical problems. As shown below, we simply have to replace  $s$  by  $j\omega$ .

$$f(s) = \int_0^\infty F(t) e^{-st} dt \quad f(j\omega) = \int_0^\infty F(t) e^{-j\omega t} dt \quad (22)$$

Laplace

Fourier

There have been a few investigations into the use of the Fast Fourier Transform but it needs further exploration. Nevertheless at the moment it appears that in order to reach the accuracy obtainable in conventional frequency response analysis, signal averaging needs to be performed. As

a result there is little or no saving in time, and so there is a question mark as to whether FFT is worthwhile for this application.<sup>63</sup>

Transient Techniques at Hydrodynamic Electrodes

Over the last few years transient techniques have been developed at solid hydrodynamic electrodes. These offer new possibilities in the evaluation of kinetic parameters. We have a known flow pattern which, owing to the forced convection, may increase the timescale of the experiment. Additionally the flow can be modulated. It has been shown that at rotating disc electrodes there exists an implicit relationship<sup>64</sup>

$$\left(\frac{\partial \omega}{\partial I}\right)_E = - \left(\frac{\partial \omega}{\partial E}\right)_I \cdot \left(\frac{\partial E}{\partial I}\right)_\omega \quad (25)$$

where

$\left(\frac{\partial \omega}{\partial I}\right)_E$  is the electrohydrodynamical impedance under potentiostatic control

$\left(\frac{\partial \omega}{\partial E}\right)_I$  is the electrohydrodynamical impedance under galvanostatic control

$\left(\frac{\partial E}{\partial I}\right)_\omega$  is the electrochemical impedance

Solution of the convective-diffusion equation is more complicated and usually it has to be obtained numerically, although an analytical approach has been used with some success.<sup>65</sup>

Some of the developments in this field are given in the following sub-sections. It is to be noted that many do not enable as yet the calculation of kinetic parameters. We also include for comparison purposes, and due to its hydrodynamic character, transient techniques at the DME.

(i) Potential Step and Pulse

Although these have been used for some years at the DME, it is only recently with the theoretical work of Los et al.<sup>66</sup> and Galvez et al.<sup>67</sup> that all the kinetic and mechanistic parameters can be evaluated.

At the RDE the current response to a potential step has been evaluated analytically and numerically: there is an inherently practical application of this research as pulsed potential leads to higher quality electro-deposition and the RDE is uniformly accessible.<sup>68</sup> At the ring electrode

of an RRDE, we will register a transient from a disc potential step affected only by the disc current's Faradaic component.

(ii) Current Step and Pulse

Providing we can separate out the double layer contribution, use of hydrodynamic electrodes increases the transition time in the Sand equation (eqn. 18) enabling more accurate measurement. Theoretical treatments which allow evaluation of kinetic parameters have appeared for the RDE<sup>69</sup> and DME<sup>70</sup> — in the latter case the current is programmed with drop growth.

At a double electrode such as the RRDE current steps at the disc can give information about disc surface processes from analysis of the resulting ring transient.<sup>71-73</sup>

(iii) Alternating Current

The thickness of the diffusion layer associated with the ac perturbation is much less than the hydrodynamic boundary layer thickness at high frequencies — the effect of convection can be neglected. At low frequencies this is no longer true: the 'transition' frequency is around 40Hz at the RDE<sup>74</sup> and 10Hz at the tubular electrode<sup>75</sup> in aqueous solution under typical conditions.

Results for mixed kinetic control and coupled homogeneous reactions are very similar at the RDE to those at the DME<sup>74</sup>. In particular the kinetic parameter evaluation in ac polarography for coupled chemical reactions relies on their very high phase-angle sensitivity: where convection can be neglected, at high frequency, the DME diagnostics and evaluation method may be directly applied.<sup>76</sup>

At double electrodes the phase shift of the ring current with respect to the disc current enables us to distinguish between the total flux of electrons and the flux of electroactive species at the disc;  $N_k$  (1st order) can be calculated.<sup>77</sup>

(iv) Linear Sweep at the RDE

In LSV at stationary electrodes there can be unwanted side effects due to natural convection and so forth. Forced convection removes this disadvantage and allows peak and limiting currents to be measured in a single experiment. Additionally there is only a weak dependence on electrolyte properties ( $v^{1/6}$ ).<sup>78</sup>

(v) Hydrodynamic Modulation at the RDE

In this type of experiment proposed originally by Bruckenstein et al.<sup>79</sup>, we modulate the rotation speed of the electrode about a central

value. Essentially we will be measuring the electrohydrodynamical impedance. The modulated current response should be free of contributions from flow independent causes i.e. surface processes, and sensitivity is thus enhanced. The whole frequency range for modulation, including large amplitude modulation has been studied.<sup>80,81</sup> Kinetic applications have still to be fully realised.

Conclusion

An electrochemist has at his disposal a varied number of techniques with which to investigate the kinetics and mechanism of electrode processes. For some of the more common techniques, an idea of the range of determinable rate constants is given in Table VII.

Table VII. Approximate Range of Measurement of Rate Constants

	cm s <sup>-1</sup>
DME	$k'_o < 10^{-4}$
RDE	$k'_o < 10^{-2}$
Pot. step <sup>a</sup>	$10^{-3} < k'_o < 10^{-1}$
Impedance <sup>a</sup>	$10^{-5} < k'_o < 1$

<sup>a</sup> The lower limit arises because of the increasing contribution from the double layer capacitance.

With modern instrumentation the techniques are becoming more complex as are the numerical solutions to and digital simulation of the convective-diffusion or diffusion equations. However, let us not allow mathematical complexity or flashing lights blind us as to what is really happening at the electrode-solution interface. A physical picture of the interface will give the answer to many questions and is, without doubt, very important for the fundamental understanding of the kinetics of the electrode process.

List of Symbols

- a diameter of impinging jet (wall-jet electrode)/cm
- A see equation 10 and Table IV
- A electrode area/cm<sup>2</sup>
- c concentration/mol cm<sup>-3</sup> or mol dm<sup>-3</sup>
- c<sub>∞</sub> concentration in bulk solution
- c<sub>o</sub> concentration at electrode surface
- C<sub>d</sub> differential double layer capacitance/μF cm<sup>-2</sup>
- d width of channel (channel electrode, Table III)/cm
- DME dropping mercury electrode
- D diffusion coefficient/cm<sup>2</sup> s<sup>-1</sup>
- E potential of electrode vs. reference electrode/V
- E<sup>⊖</sup> standard potential/V
- E<sub>eq</sub> equilibrium potential/V
- E<sub>p</sub> peak potential (eqns. 19 and 20)/V
- E<sub>1/2</sub> half-wave potential (i=[(i<sub>L</sub><sup>a</sup>+i<sub>L</sub><sup>c</sup>)/2])/V
- f function defined by eqn. 22
- F function defined by eqn. 13 or eqn. 22
- F Faraday/C mol<sup>-1</sup>
- h half-height of channel (channel electrode, Table III)/cm
- i current/mA or A
- i<sub>D</sub> disc current
- i<sub>R</sub> ring current
- i<sub>k</sub> kinetic current defined by eqn. 9
- i<sub>L</sub> diffusion-limited current
- i<sub>L</sub><sup>a</sup> diffusion-limited anodic current
- i<sub>L</sub><sup>c</sup> diffusion-limited cathodic current
- i<sub>o</sub> exchange current defined by eqn. 4a
- k homogeneous rate constant
- k' heterogeneous rate constant/cm s<sup>-1</sup>
- k'<sub>o</sub> standard heterogeneous rate constant (eqn. 3)/cm s<sup>-1</sup>
- k'<sub>D</sub> mass transfer coefficient/cm s<sup>-1</sup>
- m<sub>1</sub> flow-rate of mercury/mg s<sup>-1</sup>
- N<sub>k</sub> kinetic collection efficiency of double electrode
- N<sub>o</sub> steady-state collection efficiency of double electrode (eqn. 12)
- r radial variable

$r_1$	radius of disc electrode/cm
$r_2$	inner radius of ring electrode/cm
$r_3$	outer radius of ring electrode/cm
$r_T$	radius of tube (wall-tube electrode)/cm
$R$	radius of tube (tubular electrode)/cm
$R_{ct}$	charge-transfer resistance
RDE	rotating disc electrode
RRDE	rotating ring-disc electrode
$t_{tr}$	transition time (eqn. 18)
TDE	tube double electrode
$v$	scan rate/mV s <sup>-1</sup> or V s <sup>-1</sup>
$V_f$	volume flow rate/cm <sup>3</sup> s <sup>-1</sup>
$w$	width of channel electrode/cm
$W$	rotation speed/Hz
$x$	length variable
$x_1$	length of generator electrode (TDE)/cm
$x_2$	$x_1$ plus generator/detector electrode gap/cm
$x_3$	$x_2$ plus detector electrode/cm
$z$	distance from electrode surface/cm axial variable
$Z_w$	Warburg impedance
$\alpha$	electrochemical charge transfer coefficient geometric parameter (Table V)
$\beta$	symmetry factor geometric factor (Table V)
$\delta$	diffusion layer thickness
$\xi$	defined in eqn. 10a
$\eta$	overpotential/V
$\nu$	kinematic viscosity/cm <sup>2</sup> s <sup>-1</sup>
$\sigma$	mass transport parameter (Table IV)
$\tau$	drop time (Tables III, IV)
$\omega$	rotation speed/rad s <sup>-1</sup> frequency/Hz

## REFERENCES

1. B.E. Conway, J. Electrochem. Soc., 1977, 124, 410C-421C.
2. K.J. Vetter, "Electrochemical Kinetics", Academic Press, New York, 1967.
3. P. Delahay, "Double Layer and Electrode Kinetics", Wiley, New York, 1965.
4. W.J. Albery, "Electrode Kinetics", Clarendon Press, Oxford, 1975.
5. R.N. Adams, "Electrochemistry at Solid Electrodes", Dekker, New York, 1969.
6. A.J. Bard and L.R. Faulkner, "Electrochemical Methods: Fundamentals and Applications", Wiley, New York, 1980.
7. D.D. MacDonald, "Transient Techniques in Electrochemistry", Plenum, New York, 1977.
8. B.E. Conway, J. O'M. Bockris, E. Yeager, R.E. White and S.U.M. Khan eds., "Comprehensive Treatise of Electrochemistry. Vol.7. Kinetics and Mechanism of Electrode Processes", Plenum, New York, 1983.
9. C.H. Bamford, C.F.H. Tipper and R.G. Compton eds., "Comprehensive Chemical Kinetics. Vols. 26 and 27: Electrode Kinetics", Elsevier, Amsterdam, in press.
10. Ref. 6 Ch. 14.
11. B.H. Loo and Y.G. Lee, J. Electroanal. Chem., 1984, 163, 401-405 and references therein.
12. e.g. J. Chem. Ed. 1983, 60, 325-340.
13. W.J. Albery and A.R. Hillman, Ann. Rep. Chem. Soc. Sect. C, 1981, 73, 377-437.
14. V.G. Levich, "Physicochemical Hydrodynamics", Prentice-Hall, Englewood Cliffs, NJ, 1962.
15. J. Newman, "Electrochemical Systems", Prentice-Hall, Englewood Cliffs, NJ, 1973.
16. J.O'M. Bockris and Z. Nagy, J. Chem. Ed., 1973, 50, 839-843.
17. Ref. 4 p.79.
18. I. Ruziĉ et al., J. Electroanal. Chem., 1969, 22, 243-252; 1970, 25, 144-147; 1971, 29, 440-442; 1972, 36, 447-456; 1977, 75, 9-24.
19. R.M. Wightman, Anal. Chem., 1981, 53, 1125A-1134A.
20. M. Lovriĉ, T. Magjer and M. Branica, Croat. Chem. Acta, 1984, 57, 157-163.
21. M. Abramowitz and I. Stegun "Handbook of Mathematical Functions", Dover, New York, 1970 pp. 1019-1030.

22. S. Feldberg in "Electroanalytical Chemistry" ed. A.J. Bard, Dekker, New York, 1969, 3, 200-296.
23. D. Britz, "Digital Simulation in Electrochemistry", Springer-Verlag, Berlin, 1981.
24. C.M.A. Brett and A.M. Oliveira Brett in Ref. 9 Vol. 26 Ch. 5.
25. A.C. Riddiford, Adv. Electrochem. Eng., 1964, 4, 47-116.
26. Yu. V. Pleskov and V. Yu. Filinovskii, "The Rotating Disc Electrode", Plenum, New York, 1976.
27. F. Opekar and P. Beran, J. Electroanal. Chem., 1976, 69, 1-105.
28. A.N. Frumkin and L.I. Nekrasov, Dokl. Akad. Nauk SSSR, 1959, 126, 115-118.
29. W.J. Albery and M.L. Hitchman, "Ring-Disc Electrodes", Clarendon Press, Oxford, 1971.
30. S. Bruckenstein and B. Miller, Acc. Chem. Res., 1977, 10, 54-61.
31. J. Heyrovský, Chem. Listy, 1922, 16, 256.
32. I.M. Kolthoff and J.J. Lingane "Polarography" 2nd ed., Wiley, New York, 1952.
33. R. Brdička, V. Hanuš and J. Koutecký, "Progress in Polarography" ed. P. Zuman and I.M. Kolthoff, 1962, 1, 145-199.
34. D. Ilkovič, Coll. Czech. Chem. Commun., 1934, 6, 498-513.
35. W.J. Albery and S. Bruckenstein, J. Electroanal. Chem., 1983, 144, 105-112.
36. Ref. 14 p. 112 et seq.
37. J. Yamada and H. Matsuda, J. Electroanal. Chem., 1973, 44, 189-198.
38. W.J. Albery and C.M.A. Brett, J. Electroanal. Chem., 1983, 148, 201-210.
39. e.g. D. Jahn and W. Vielstich, J. Electrochem. Soc., 1962, 109, 849-852.
40. Ref. 14 p. 74.
41. J. Koutecký and V.G. Levich, Dokl. Akad. Nauk. SSSR, 1957, 117, 441-444.
42. H. Matsuda, J. Electroanal. Chem., 1972, 35, 77-84.
43. K. Tokuda and H. Matsuda, J. Electroanal. Chem., 1973, 44, 199-212.
44. W.J. Albery, S. Bruckenstein and D.T. Napp, Trans. Faraday Soc., 1966, 62, 1932-1937.
45. H. Matsuda, J. Electroanal. Chem., 1967, 15, 325-336.
46. L.N. Klatt and W.J. Blaedel, Anal. Chem., 1967, 39, 1065-1072.
47. H. Matsuda and Y. Ayabe, Bull. Chem. Soc. Japan, 1954, 28, 422-428.
48. K.-L. Hsueh, D.T. Chin and S. Srinivasan, J. Electroanal. Chem.,

- 1983, 153, 79-95 and references therein.
49. Ref. 29 Chs. 8 and 9.
50. K. Aoki, K. Tokuda and H. Matsuda, J. Electroanal. Chem., 1977, 79, 49-78.
51. K. Aoki and H. Matsuda, J. Electroanal. Chem., 1978, 94, 157-163.
52. F.G. Cottrell, Z. Physik. Chem., 1902, 42, 385-431.
53. Ref. 7 Ch.4.
54. H.J.S. Sand, Phil. Mag., 1901, 1, 45.
55. Ref. 7 Ch.5.
56. R.S. Nicholson and I. Shain, Anal. Chem., 1964, 36, 706-723.
57. R.S. Nicholson, Anal. Chem., 1965, 37, 1351-1355.
58. J.M. Saveant et al., J. Electroanal. Chem., 1973, 44, 169-187; 1973, 47, 215-221; 1974, 52, 403-412; 1975, 61, 251-263; 1975, 65, 57-66.
59. K.B. Oldham, Anal. Chem., 1972, 44, 196-198.
60. M. Grenness and K.B. Oldham, Anal. Chem., 1972, 44, 1121-1129.
61. M. Sluyters-Rehbach and J.H. Sluyters in "Electroanalytical Chemistry" ed. A.J. Bard, Dekker, New York, 1970, 4, 1-128.
62. D.D. MacDonald and M.C.H. McKubre in "Modern Aspects of Electrochemistry" ed. J.O'M. Bockris, B.E. Conway and R.E. White, Plenum, New York, 1982, 14, 61-150.
63. C. Gabrielli, F. Huet, M. Keddam and J.F. Lizée, J. Electroanal. Chem., 1982, 138, 201-208.
64. C. Deslouis, I. Epelboin, C. Gabrielli, Ph. Saint-Rose Fanchine and B. Tribollet, J. Electroanal. Chem., 1980, 107, 193-195.
65. C. Deslouis, C. Gabrielli and B. Tribollet, J. Electrochem. Soc., 1983, 130, 2044-2046.
66. L.F. Roeleveld, B.J.C. Wetsema and J.M. Los, J. Electroanal. Chem., 1977, 75, 839-844 and references therein.
67. J. Gálvez, A. Molina and C. Serna, J. Electroanal. Chem., 1981, 124, 201-211 and references therein.
68. K. Viswanathan and H.Y. Cheh, J. Appl. Electrochem., 1979, 9, 537-543, and references therein.
69. J.M. Hale, J. Electroanal. Chem., 1963, 6, 187-197; 1964, 8, 332-349.
70. H.L. Kies, J. Electroanal. Chem., 1973, 45, 71-77; 1977, 76, 1-17.
71. Ref. 29 pp. 149-151.
72. S. Bruckenstein, A. Tokuda and W.J. Albery, J. Chem. Soc. Faraday Trans. I., 1977, 73, 823-829.
73. W.J. Albery, M.G. Boutelle, P.J. Colby and A.R. Hillman, J. Chem. Soc. Faraday Trans. I., 1982, 78, 2757-2763.

74. K. Tokuda and H. Matsuda, J. Electroanal. Chem., 1977, 82, 157-171; 1978, 90, 149-163; 1979, 95, 147-157.
75. R.G. Compton and G.R. Sealy, J. Electroanal. Chem., 1983, 145, 35-41.
76. D.E. Smith in "Electroanalytical Chemistry" ed. A.J. Bard, Dekker, New York, 1966, 1, 1-155.
77. W.J. Albery et al., J. Chem. Soc. Faraday Trans I., 1971, 67, 2414-2418; 1978, 74, 1007-1019; 1979, 75, 1623-1634.
78. H.Y. Cheh et al., J. Electrochem. Soc., 1980, 127, 2153-2157, 2385-2388; J. Electroanal. Chem., 1981, 124, 95-101; 1983, 144, 77-85.
79. S. Bruckenstein, M.I. Bellavance and B. Miller, J. Electrochem. Soc., 1973, 120, 1351-1356.
80. C. Deslouis, C. Gabrielli, Ph. Sainte-Rose Fanchine and B. Tribollet, J. Electrochem. Soc., 1982, 129, 107-118.
81. B. Tribollet and J. Newman, J. Electrochem. Soc., 1983, 130, 2016-2026.

DETERMINATION OF STABILITY CONSTANTS USING ASV TECHNIQUE  
(SURFACE CONCENTRATION EFFECT)

J. Buffle<sup>\*</sup>, A.M. Mota<sup>\*\*</sup>, M.L. Gonçalves<sup>\*\*</sup>

<sup>\*</sup>Department of Analytical Chemistry  
University of Geneva, Sciences II  
1211 Geneva 4, Switzerland

<sup>\*\*</sup>Centro de Química Estrutural  
Complexo I, Instituto Superior Técnico  
1096 Lisboa Codex, Portugal

ABSTRACT

The surface concentration effect of the metal ion during the stripping step of ASV, in a complexing medium, is discussed in terms of determination of stability constants, from the results for Pb(II) + TETA system.

Subsequently stability constants of Cd(II) + carboxyphenyliminodiacetic acid, phenylmethyyliminodiacetic acid, pyridine-2,6-dicarboxylic acid and pyridine-2-carboxylic acid have been determined and the values compared with those obtained by other techniques.